



THE UNIVERSITY *of* EDINBURGH

## Edinburgh Research Explorer

### Elliptical instability of a rapidly rotating, strongly stratified fluid

**Citation for published version:**

Aspden, JM & Vanneste, J 2009, 'Elliptical instability of a rapidly rotating, strongly stratified fluid', *Physics of Fluids*, vol. 21, no. 7, 074104, pp. -. <https://doi.org/10.1063/1.3177354>

**Digital Object Identifier (DOI):**

[10.1063/1.3177354](https://doi.org/10.1063/1.3177354)

**Link:**

[Link to publication record in Edinburgh Research Explorer](#)

**Document Version:**

Publisher's PDF, also known as Version of record

**Published In:**

Physics of Fluids

**General rights**

Copyright for the publications made accessible via the Edinburgh Research Explorer is retained by the author(s) and / or other copyright owners and it is a condition of accessing these publications that users recognise and abide by the legal requirements associated with these rights.

**Take down policy**

The University of Edinburgh has made every reasonable effort to ensure that Edinburgh Research Explorer content complies with UK legislation. If you believe that the public display of this file breaches copyright please contact [openaccess@ed.ac.uk](mailto:openaccess@ed.ac.uk) providing details, and we will remove access to the work immediately and investigate your claim.



## Elliptical instability of a rapidly rotating, strongly stratified fluid

J. M. Aspden and J. Vanneste

Citation: [Phys. Fluids](#) 21, 074104 (2009); doi: 10.1063/1.3177354

View online: <http://dx.doi.org/10.1063/1.3177354>

View Table of Contents: <http://pof.aip.org/resource/1/PHFLE6/v21/i7>

Published by the [American Institute of Physics](#).

---

### Additional information on Phys. Fluids

Journal Homepage: <http://pof.aip.org/>

Journal Information: [http://pof.aip.org/about/about\\_the\\_journal](http://pof.aip.org/about/about_the_journal)

Top downloads: [http://pof.aip.org/features/most\\_downloaded](http://pof.aip.org/features/most_downloaded)

Information for Authors: <http://pof.aip.org/authors>

### ADVERTISEMENT



**Running in Circles Looking  
for the Best Science Job?**

**Search hundreds of exciting  
new jobs each month!**

<http://careers.physicstoday.org/jobs>

**physicstodayJOBS**



# Elliptical instability of a rapidly rotating, strongly stratified fluid

J. M. Aspden and J. Vanneste

*School of Mathematics and Maxwell Institute for Mathematical Sciences, University of Edinburgh, Edinburgh EH9 3JZ, United Kingdom*

(Received 2 February 2009; accepted 6 June 2009; published online 15 July 2009)

The elliptical instability of a rotating stratified fluid is examined in the regime of a small Rossby number and order-one Burger number corresponding to rapid rotation and strong stratification. The Floquet problem describing the linear growth of disturbances to an unbounded, uniform-vorticity elliptical flow is solved using exponential asymptotics. The results demonstrate that the flow is unstable for arbitrarily strong rotation and stratification; in particular, both cyclonic and anticyclonic flows are unstable. The instability is weak, however, with growth rates that are exponentially small in the Rossby number. The analytic expression obtained for the growth rate elucidates its dependence on the Burger number and on the eccentricity of the elliptical flow. It explains, in particular, the weakness of the instability of cyclonic flows, with growth rates that are only a small fraction of those obtained for the corresponding anticyclonic flows. The asymptotic results are confirmed by numerical solutions of the Floquet problem. © 2009 American Institute of Physics. [DOI: 10.1063/1.3177354]

## I. INTRODUCTION

Elliptical instability, the three-dimensional instability of two-dimensional flows with elliptical streamlines, has been the focus of a great deal of research activity. The review in Ref. 1 discusses the main results up to 2002 and emphasizes the relevance of elliptical instability to a broad range of applications. One of these is the instability of two-dimensional vortices that are deformed elliptically by a large-scale strain flow. This is especially important for the dynamics of the atmosphere and ocean since this is characterized by an abundance of vortices that are deformed through either mutual interactions or the effect of large-scale flows. In this context, however, the planetary rotation and density stratification need to be taken into account.

Rotation and stratification clearly exert a strong influence on elliptical instability: Since this stems from the parametric resonance between the periodic fluctuations associated with the elliptical motion and the free waves supported by the flow, the dispersion relation of these waves is critical. In the presence of both rotation and stratification, the waves are inertia-gravity waves whose frequency is bounded from below by the minimum of the Coriolis parameter  $f$  and Brunt–Väisälä frequency  $N$ . As a consequence, a vortex of fixed vorticity ceases to be unstable by the subharmonic instability responsible for the simplest form of elliptical instability when both  $f$  and  $N$  exceed a certain threshold. As these parameters increase further, instabilities are limited to resonances of higher and higher order, leading to decreasing growth rates. This was clearly demonstrated by Miyazaki<sup>2</sup> on the basis of numerical solutions of the Floquet problem that models elliptic instability (see also Refs. 1 and 3). Further numerical results were obtained by McWilliams and Yavneh,<sup>4</sup> who concentrated on the regime of rapid rotation and strong stratification with  $N > f$  most relevant to the atmosphere and ocean. Their broad motivation was the role that instabilities play in the generation of inertia-gravity-

wave-like motion, and the resulting breakdown of the nearly geostrophic and hydrostatic balance that is typical of much of the atmosphere and ocean. The present paper shares the same motivation. It re-examines the elliptical instability of a rotating stratified fluid and derives explicit analytical results in the limit of fast rotation  $f \gg \Omega$  and strong stratification  $N \gg \Omega$ , where  $\Omega$  denotes the (relative) vorticity of the flow.

Several recent papers<sup>5–8</sup> have demonstrated in specific examples that instabilities of well-balanced basic flows to inertia-gravity-wave perturbations (or perturbations related to similar fast waves) have growth rates that are exponentially small in the Rossby number, here proportional to  $\Omega/f \ll 1$ .<sup>9</sup> Theoretical arguments<sup>10,11</sup> indicate that this is a generic property, and the elliptical instability examined in this paper is no exception. In this case, the exponential smallness can be roughly understood by noting that in the manner typical of parametric instabilities,<sup>12</sup> the growth rates of the elliptical instability can be expected to be proportional to  $\Omega^n$ , where  $n$  is the order of the resonance. Since, as pointed out by Miyazaki,<sup>2</sup> the minimum  $n$  is of the order  $f/\Omega$  (for  $N > f$ ), this leads to the conclusion that growth rates are beyond all orders in the Rossby number. To go further than this rough argument and provide an estimate for the growth rate requires the exponential-asymptotics analysis of the Floquet problem relevant to the elliptical instability. We carry out this analysis and, rather than relying on general asymptotic results for Hill's equations,<sup>13</sup> directly relate the growth of solutions to the occurrence of a Stokes phenomenon<sup>14</sup> which we capture using a combination of WKB expansion and matched asymptotics in complex time. The analytical results are confirmed by the numerical solutions of the Floquet problem.

One of the issues which our treatment clarifies is the difference between the instability of cyclonic and anticyclonic vortices in the presence of both rapid rotation and strong stratification. Cyclones have been recognized as less

unstable than anticyclones, to the extent that McWilliams and Yavneh<sup>4</sup> considered only the instability of the latter. We show that the cyclones are in fact linearly unstable, with growth rates that have the same exponential dependence on the Rossby number as the corresponding anticyclones but differ by a factor which, although formally of order one, turns out to be numerically very small.

The plan of this paper is as follows. In Sec. II, we formulate the problem of elliptical instability in a rotating stratified fluid modeled using the Boussinesq approximation. We use the simplest instance of elliptical instability, that of an unbounded elliptical vortex with uniform vorticity. This makes it possible to seek global solutions in the form of plane waves with time-periodic wavevector and an amplitude that satisfies Hill's equation. (Results for this particular case have a much broader appeal, however, since an identical Hill's equation arises when the stability of more general elliptical vortices is examined locally using the geometric-optics technique.<sup>15–17</sup>) The Floquet problem associated with Hill's equation is solved asymptotically in Sec. III in the limit of fast rotation and strong stratification, with the eccentricity of the elliptical streamlines assumed of order one. For simplicity, we also make the hydrostatic approximation assuming that  $N \gg f$  and an order-one Burger number. The asymptotic derivation is only sketched in Sec. III, with technical details relegated to Appendix A. The asymptotic results are confirmed by direct numerical solution of the Floquet problem in Sec. IV. The effect of a finite  $N/f$  is also briefly examined there.

## II. FORMULATION

We consider the stability of a horizontal elliptical flow in a three-dimensional stratified fluid, with constant Brunt-Väisälä frequency  $N$ , rotating about the vertical axis at rate  $f/2 > 0$ . The flow's streamfunction, velocity, and vorticity are written as

$$\Psi = -\frac{1}{2}(bx^2 + ay^2), \quad \mathbf{U} = (ay, -bx, 0), \quad \text{and} \quad \Omega = -(a + b), \quad (2.1)$$

where  $ab > 0$ . We define

$$s = \text{sgn } a = \text{sgn } b$$

and note that the flow is anticyclonic for  $s=1$ , and cyclonic for  $s=-1$ . Three dimensionless parameters characterize the flow, namely,

$$e = \sqrt{a/b}, \quad \epsilon = \sqrt{ab}/f, \quad \text{and} \quad f/N, \quad (2.2)$$

which are recognized as the aspect ratio of the elliptical flow, a Rossby number, and the Prandtl ratio. We assume that  $e > 1$  without loss of generality.

Perturbations to the flow (2.1) take the form of plane waves with time-dependent wavevector, with each field written as

$$u(\mathbf{x}, t) = \hat{u}(t)e^{i\mathbf{k}(t) \cdot \mathbf{x}}, \quad (2.3)$$

where the wavevector  $\mathbf{k} = (k, l, m)$  satisfies

$$\dot{k} = bl, \quad \dot{l} = -ak, \quad \text{and} \quad \dot{m} = 0, \quad (2.4)$$

the overdot denoting differentiation with respect to  $t$ . In what follows, we use a dimensionless time variable obtained by taking  $(ab)^{-1/2}$  as a reference time. In terms of this variable, the solutions to Eq. (2.4) have the simple form

$$k = k_0 \cos t, \quad l = -s\epsilon k_0 \sin t, \quad \text{and} \quad m = m_0, \quad (2.5)$$

where  $k_0$  and  $m_0$  are constant. The stability of Eq. (2.1) depends on the behavior of the amplitudes  $\hat{u}(t)$ ,  $\hat{v}(t)$ , etc., as  $t \rightarrow \infty$ . These satisfy a set of ordinary differential equations with time-periodic coefficients. Following McWilliams and Yavneh,<sup>4</sup> this set can be conveniently reduced to a single second-order equation for the amplitude of the vertical component of the vorticity  $\hat{\zeta} = i(l\hat{v} - k\hat{u})$ . See Appendix A for details. Assuming that the perturbation potential vorticity vanishes, this equation reduces to

$$\ddot{\zeta} + \frac{2sklm^2(e - e^{-1})}{\kappa^2(k^2 + l^2)}\dot{\zeta} + \frac{1}{\epsilon^2} \left\{ \left[ 1 - s\epsilon(e + e^{-1}) \left( 1 - \frac{2s\epsilon\epsilon k_0^2}{k^2 + l^2} \right) \frac{m^2}{\kappa^2} + \frac{N^2(k^2 + l^2)}{f^2\kappa^2} \right] \right\} \zeta = 0, \quad (2.6)$$

where  $\kappa^2 = k^2 + l^2 + m^2$  and we have omitted the hat on the amplitude  $\zeta$ . Four dimensionless parameters appear in this equation: the three flow parameters (2.2), and the initial aspect ratio  $m_0/k_0$  of the perturbation.

Most of this paper focuses on a limiting case of Eq. (2.6) obtained by making the hydrostatic approximation. This assumes that  $m_0 \gg k_0$  and  $N \gg f$  while

$$\mu = \frac{fm_0}{Nk_0} = O(1). \quad (2.7)$$

This is the regime most relevant to the dynamics of the atmosphere and oceans since the condition  $N \gg f$  is verified while, as we demonstrate below, the largest growth rates of the elliptical instability correspond to  $\mu = O(1)$ . The parameter  $\mu$  can be recognized as the inverse square root of a Burger number; it can be interpreted as the aspect ratio of the perturbation scaled by  $f/N$  as is natural in rapidly rotating, strongly stratified fluids.

In the hydrostatic approximation,  $\kappa^2$  is approximated by  $m^2$ , and Eq. (2.6) reduces to

$$\ddot{\zeta} + \frac{2skl(e - e^{-1})}{k^2 + l^2}\dot{\zeta} + \frac{1}{\epsilon^2} \left\{ \left[ 1 - s\epsilon(e + e^{-1}) \left( 1 - \frac{2s\epsilon\epsilon k_0^2}{k^2 + l^2} \right) + \frac{N^2(k^2 + l^2)}{f^2m^2} \right] \right\} \zeta = 0. \quad (2.8)$$

Using Eq. (2.5) and defining  $\psi > 0$  by

$$e^2 = 1 + \psi^2, \quad (2.9)$$

we rewrite this equation as



$$\ddot{\zeta} - p(t)\dot{\zeta} + \frac{1}{2}[\omega^2(t) - \epsilon q(t) + \epsilon^2 r(t)]\zeta = 0. \quad (2.10)$$

Here

$$\omega^2 = 1 + \frac{N^2(k^2 + l^2)}{f^2 m^2} = 1 + \mu^{-2}(1 + \psi^2 \sin^2 t) \quad (2.11)$$

can be recognized as the square of the inertia-gravity-wave frequency (nondimensionalized by  $f$ ). We have also introduced

$$p(t) = \frac{\psi^2 \sin(2t)}{1 + \psi^2 \sin^2 t}, \quad q(t) = \varsigma \left( e + e^{-1} + \frac{2e}{1 + \psi^2 \sin^2 t} \right), \quad (2.12)$$

$$\text{and } r(t) = \frac{2(e^2 + 1)}{1 + \psi^2 \sin^2 t}.$$

Equation (2.10) is a Hill equation, with coefficients that are  $\pi$ -periodic in  $t$ . Its stability is determined using the Floquet theory for Hill equations.<sup>12</sup> We briefly recall the main result of this theory. Let  $\zeta_1(t)$  and  $\zeta_2(t)$  denote two linearly independent solutions of Eq. (2.10), and let us form the column vector  $\zeta(t) = [\zeta_1(t), \zeta_2(t)]^T$ . The  $\pi$ -periodicity of the coefficients in Eq. (2.10) implies that

$$\zeta(t + \pi) = M\zeta(t)$$

for some constant matrix  $M$ . The eigenvalues  $\lambda$  of  $M$  are then the Floquet multipliers, and two fundamental solutions can be found for which

$$\zeta(t) = e^{\sigma t} \phi(t), \quad (2.13)$$

where

$$\sigma = \frac{1}{\pi} \log \lambda \quad (2.14)$$

is the Floquet exponent, and  $\phi(t)$  is  $\pi$ -periodic. Note that the form of the coefficient of  $\dot{\zeta}$  ensures that the two multipliers satisfy  $\lambda_1 \lambda_2 = 1$ . Instability occurs when one of these is such that  $|\lambda| > 1$  or, equivalently,  $\text{Re } \sigma > 0$ . The matrix  $M$  is computed by relating  $\zeta$  and  $\dot{\zeta}$  at two times  $t$  and  $t + \pi$ . Here we choose  $t = -\pi/2$  and compute  $M$  as

$$M = [\zeta(\pi/2), \dot{\zeta}(\pi/2)][\zeta(-\pi/2), \dot{\zeta}(-\pi/2)]^{-1}. \quad (2.15)$$

Our aim is to determine the largest values of the growth rate  $\text{Re } \sigma$  for Eq. (2.10) analytically in the fast-rotation regime  $\epsilon \ll 1$ , with  $N \gg f$ ,  $\mu = O(1)$ , and  $\psi = O(1)$ . In this regime Eq. (2.10) resembles the Hill equations with large parameters whose stability was studied by Weinstein and Keller<sup>13</sup> using a mapping to parabolic cylinder functions. However, there are difficulties in applying their results directly, related to the presence of a first derivative term that is singular for the complex values of  $t$  such that  $k^2 + l^2 = 0$ . We have therefore found it simpler to develop a different approach, combining WKB analysis with complex-time matching. This approach, which has the advantage of demonstrating the link between the instability and the Stokes phenomenon,<sup>14,18</sup> is described

in Sec. III and in Appendix B. The analytic results obtained there are confirmed and extended to finite  $N/f$  in Sec. IV by solving Eq. (2.10) numerically.

### III. WKB ANALYSIS

A WKB solution of the form

$$\zeta(t) = A(t)e^{i\theta(t)/\epsilon} \quad (3.1)$$

can be introduced into Eq. (2.10) and the (real) functions  $A(t)$  and  $\theta(t)$  can be sought as the asymptotic series

$$A = A_0 + \epsilon A_1 + \cdots \quad \text{and} \quad \theta = \theta_0 + \epsilon \theta_1 + \cdots. \quad (3.2)$$

Introducing Eqs. (3.1) and (3.2) into Eq. (2.10), we find at leading order that

$$\theta_0(t) = \int_{-\pi/2}^t \omega(t') dt'. \quad (3.3)$$

At the next order, we have

$$\frac{\dot{A}_0}{A_0} = -\frac{\dot{\omega}}{2\omega} + \frac{p}{2}, \quad (3.4)$$

$$\dot{\theta}_1 = -\frac{q}{2\omega}. \quad (3.5)$$

We note that  $A_0(t)$  is  $\pi$ -periodic since  $p(t)$  has zero mean in  $[-\pi/2, \pi/2]$ . Pursuing the computation to higher orders suggests that all the  $A_n(t)$ ,  $n=0, 1, \dots$  are  $\pi$ -periodic. This can be confirmed by considering the Wronskian of the pair of solutions

$$\zeta = A(t)e^{i\theta(t)/\epsilon} \quad \text{and} \quad \bar{\zeta} = A(t)e^{-i\theta(t)/\epsilon}. \quad (3.6)$$

This function, defined by  $W = \dot{\zeta}\bar{\zeta} - \zeta\dot{\bar{\zeta}} = 2i\epsilon^{-1}A^2\dot{\theta}$ , satisfies  $\dot{W} = pW$  and hence is  $\pi$ -periodic. Now, the recurrence relations for  $A_n$  and  $\theta_n$  [of which Eqs. (3.4) and (3.5) are the first terms] give  $\dot{\theta}_n$  in terms of periodic functions and the  $A_m$  for  $m < n$ . The periodicity of the  $A_n$  then follows inductively from that of the Wronskian.

The periodicity of the asymptotic series for  $A(t)$  implies that there is no instability to any algebraic order in  $\epsilon$ . To all algebraic orders, the fundamental solutions are given by Eq. (3.6) and the Floquet multipliers are simply  $\lambda = \exp[\pm i\theta(\pi/2)]$  [taking  $\theta(-\pi/2) = 0$ ] and satisfy  $|\lambda| = 1$ . Any instability is necessarily due to exponentially small effects. To capture the instability and estimate its growth rate, we therefore need to go beyond the standard WKB analysis and examine how exponentially small terms alter the form (3.6) of the solutions. These terms arise through a Stokes phenomenon associated with the presence of complex turning points, that is, complex values of  $t$  for which  $\omega(t) = 0$ . From these points emanate lines of the complex  $t$ -plane, termed Stokes lines, across which solutions defined by asymptotic series such as Eq. (3.2) acquire an additional exponentially small multiple of other linearly independent solutions. (See Refs. 19–22 for the analysis of the Stokes phenomenon in a variety of problems.)

Since the matrix  $M$  in Eq. (2.15) depends only on the solution vector  $\zeta$  at  $t = \pm \pi/2$ , the only Stokes lines relevant to our problem are those crossing the real  $t$ -axis between  $-\pi/2$  and  $\pi/2$ . As explained in Appendix B, there is only one such line, namely (a segment of) the line  $\text{Re } t = 0$ . Across this line, the asymptotic solutions  $\zeta$  and  $\bar{\zeta}$  in Eq. (3.6) switch on an exponentially small multiple of  $\bar{\zeta}$  and  $\zeta$ , respectively. More specifically, Eq. (3.6) defines a pair of independent solutions that is valid for  $-\pi/2 \leq t < -\delta$ , for some  $\epsilon^{1/2} \ll \delta \ll 1$ . When crossing  $\text{Re } t = 0$ , these solutions gain additional terms; for  $\delta < t \leq \pi/2$ , they become

$$\zeta = A(t)[e^{i\theta(t)/\epsilon} + S e^{-i\theta(t)/\epsilon}] \quad \text{and} \quad \bar{\zeta} = A(t)[e^{-i\theta(t)/\epsilon} + \bar{S} e^{i\theta(t)/\epsilon}], \quad (3.7)$$

where  $S$  is an exponentially small constant. This constant, the

Stokes multiplier, is computed in Appendix B and its modulus is given explicitly in Eq. (3.12) below. Note that  $A(t)$  and  $\theta(t)$  appearing in Eqs. (3.6) and (3.7) are defined by the asymptotic series (3.2), which diverge and must be truncated. The theory of the Stokes phenomenon<sup>19</sup> shows that optimal truncation, in which the series are truncated near their smallest term, leads to truncation errors that are asymptotically smaller than the Stokes multiplier  $S$ . Thus Eqs. (3.6) and (3.7) can be interpreted consistently by regarding  $A(t)$  and  $\theta(t)$  as defined by their asymptotic series truncated optimally. We adopt this interpretation and carry out our analysis neglecting all  $o(S)$  terms.

The Stokes multiplier  $S$  turns out to determine completely the leading-order form of the maximum growth rate of the instability. To show this, we compute the matrix  $M$  in Eq. (2.15) taking  $\zeta = (\zeta, \bar{\zeta})^T$ . We first have that

$$[\zeta(\pi/2), \dot{\zeta}(\pi/2)] = \begin{pmatrix} A(e^{i\theta/\epsilon} + S e^{-i\theta/\epsilon}) & (i\epsilon^{-1}\dot{\theta}A + \dot{A})e^{i\theta/\epsilon} + S(-i\epsilon^{-1}\dot{\theta}A + \dot{A})e^{-i\theta/\epsilon} \\ A(e^{-i\theta/\epsilon} + \bar{S} e^{i\theta/\epsilon}) & (-i\epsilon^{-1}\dot{\theta}A + \dot{A})e^{-i\theta/\epsilon} + \bar{S}(i\epsilon^{-1}\dot{\theta}A + \dot{A})e^{i\theta/\epsilon} \end{pmatrix},$$

where  $A$ ,  $\dot{A}$ ,  $\theta$ , and  $\dot{\theta}$  are evaluated at  $t = \pi/2$ . Similarly,

$$[\zeta(-\pi/2), \dot{\zeta}(-\pi/2)] = \begin{pmatrix} A & i\epsilon^{-1}\dot{\theta}A + \dot{A} \\ A & -i\epsilon^{-1}\dot{\theta}A + \dot{A} \end{pmatrix}.$$

Here  $A$ ,  $\dot{A}$ , and  $\dot{\theta}$  can be evaluated at  $t = \pi/2$ , as above, since these functions (defined by their optimally truncated series expansion) are  $\pi$ -periodic. Computing Eq. (2.15) gives the simple result

$$M = \begin{pmatrix} e^{i\theta/\epsilon} & S e^{-i\theta/\epsilon} \\ \bar{S} e^{i\theta/\epsilon} & e^{-i\theta/\epsilon} \end{pmatrix}. \quad (3.8)$$

Here  $\theta = \theta(\pi/2)$  or, more generally,  $\theta = \theta(\pi/2) - \theta(-\pi/2)$  which accommodates any convention for the arbitrary choice of  $\theta(-\pi/2)$ .

It is now readily checked that up to  $o(S)$  errors, the Floquet multipliers, that is, the eigenvalues  $\lambda$  of Eq. (3.8), satisfy  $|\lambda| = 1$  unless  $M$  is degenerate or nearly degenerate, in the sense that  $\exp(i\theta) = \exp(-i\theta) + O(S)$ . Thus the condition for instability  $|\lambda| > 1$  requires that  $\exp(i\theta)$  is exponentially close to  $\pm 1$ .<sup>23</sup> We therefore suppose that the parameters  $e$ ,  $\mu$ , and  $\epsilon$  are such that

$$e^{i\theta/\epsilon} = \pm (1 + iT) + o(S) \quad (3.9)$$

for some  $T \in \mathbb{R}$  of a similar order of magnitude as  $S$ . The Floquet multipliers obtained from Eq. (3.8) are then given by

$$\lambda = \pm (1 + \sqrt{|S|^2 - T^2}) + o(S) \quad \text{and} \quad (3.10)$$

$$\lambda = \pm (1 - \sqrt{|S|^2 - T^2}) + o(S).$$

Clearly, one of these multipliers satisfies  $|\lambda| > 1$ , and the flow is unstable, provided that  $-|S| \leq T \leq |S|$ , that is, in exponentially narrow instability bands. The corresponding growth rate  $\sigma = \sqrt{|S|^2 - T^2}/\pi + o(S)$  is maximum at the center of these bands, for  $T = 0$ , and is given by

$$\sigma_{\max} \sim \frac{|S|}{\pi}. \quad (3.11)$$

The computation of  $S$  is carried out in Appendix B. There we show that

$$|S| = e^{-\alpha/\epsilon + \beta}, \quad (3.12)$$

where

$$\alpha = \frac{2}{\mu} \int_0^{\sqrt{1+\mu^2/\psi}} \sqrt{\frac{1+\mu^2-\psi^2 x^2}{1+x^2}} dx \quad (3.13)$$

and

$$\beta = \mu \int_0^{\sqrt{1+\mu^2/\psi}} \left( e + e^{-1} + \frac{2e}{1-\psi^2 x^2} \right) \times \frac{dx}{\sqrt{(1+\mu^2-\psi^2 x^2)(1+x^2)}}. \quad (3.14)$$

Here  $\int$  denotes the Cauchy principal value of the integral, whose integrand is singular at  $x = 1/\psi$ .

Figure 1 shows the values of  $\alpha$  and  $\beta$  as functions of  $e$  and  $\mu$ . Some conclusions can be drawn from the figure and

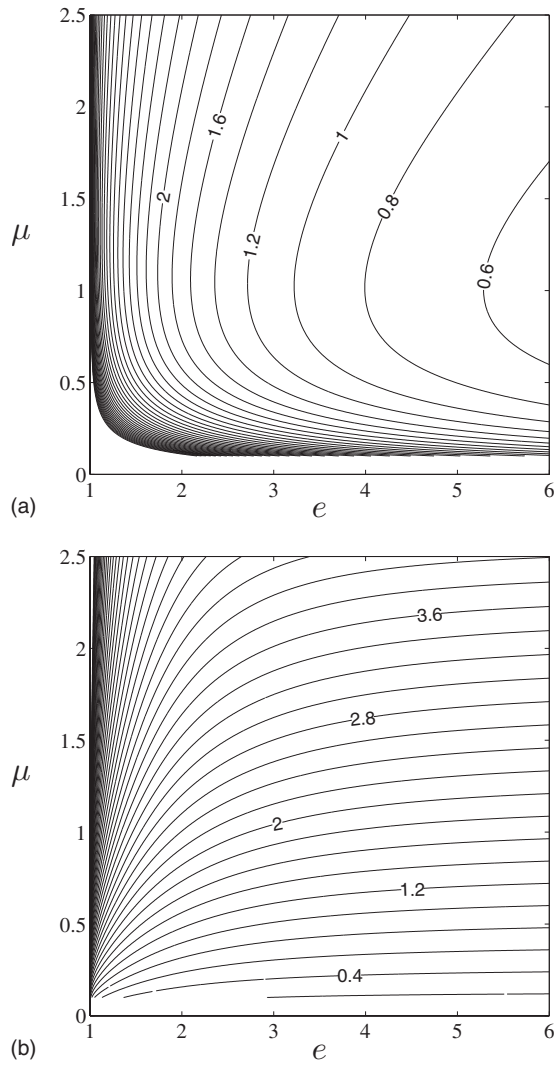


FIG. 1. Parameters  $\alpha$  and  $\beta$  governing the maximum growth rates according to Eqs. (3.11) and (3.12) as functions of  $e$  and  $\mu$ .

the examination of the explicit expressions (3.13) and (3.14). First,  $\alpha \rightarrow \infty$  in the limits of both small and large  $\mu$ ; specifically  $\alpha = O(\mu^{-1})$  as  $\mu \rightarrow 0$  and  $\alpha = O(\log \mu)$  as  $\mu \rightarrow \infty$ . This suggests, as is confirmed by Fig. 1, that the largest growth rates are attained for  $\mu = O(1)$ . Thus, the aspect ratio of the perturbations that grow as a result of the elliptical instability of vortices should be expected to be the Prandtl ratio:  $m_0/k_0 = O(N/f)$ . Second, the behavior of  $\alpha$  for small and large eccentricity is given by

$$\alpha \sim -\frac{2\sqrt{1+\mu^2}}{\mu} \left[ \log \psi + 1 - 2 \log 2 - \frac{1}{2} \log(1+\mu^2) \right] \quad \text{as } \psi \rightarrow 0, \quad (3.15)$$

$$\alpha \sim \frac{(1+\mu^2)\pi}{2\mu\psi} \quad \text{as } \psi \rightarrow \infty. \quad (3.16)$$

The large- $\psi$  expression (3.16) can actually be used to estimate  $\alpha$  for values of  $\psi$  as small as 1, which makes it very useful. [For  $\mu=1$ , for instance, the errors in Eq. (3.16) are 15%, 10%, and 5% for  $\psi=1, 1.5$ , and 2, respectively.] This

expression shows, in particular, that the largest growth rates are attained precisely for  $\mu \sim 1$  when  $\psi$  is large. Third, the obvious fact that  $\beta > 0$  shows that anticyclonic flows ( $\varsigma=1$ ) are more unstable than cyclonic flows ( $\varsigma=-1$ ). According to Eq. (3.12), the growth rate in an anticyclonic flow is a factor  $\exp(2\beta)$  larger than the growth rate of the corresponding cyclonic flow. Formally, this is an  $O(1)$  factor, but the typical values of  $\beta$  are such that it is numerically very small so that the instability of cyclones is exceedingly weak and probably negligible in most circumstances. Note that because  $\beta$  is a decreasing function of  $e$ , the asymmetry between cyclones and anticyclones is the largest for small eccentricity.

Formulas (3.11)–(3.14) give completely explicitly expressions for the maximum growth rates of the elliptical instability in terms of the three parameters  $\epsilon$ ,  $\mu$  and  $e$  (recall that  $\psi = \sqrt{e^2 - 1}$ ). These growth rates are achieved when the three parameters are related in such a way that  $\exp(i\theta/\epsilon) = \pm 1$ , that is,

$$\theta = n\pi\epsilon, \quad n = 1, 2, \dots \quad (3.17)$$

This condition can be recognized as a resonance condition between the phase of the inertia-gravity oscillations and the period of rotation around the elliptical vortex ( $2\pi$  in the dimensionless time used here).

The growth rates can be written more directly in terms of  $\epsilon$ ,  $\mu$ , and  $e$  by solving Eq. (3.17) perturbatively, with  $\theta = \theta_0 + \epsilon\theta_1 + \dots$ , and  $\theta_0$  and  $\theta_1$  obtained from Eqs. (3.3) and (3.5). This gives the approximate position of the instability bands as well as their width. To leading order, the instability bands are centered at values of  $e$  and  $\mu$  satisfying

$$\begin{aligned} \theta_0 &= \frac{1}{\mu} \int_{-\pi/2}^{\pi/2} \sqrt{1 + \mu^2 + \psi^2 \sin^2 t} dt \\ &= \frac{2}{\mu} \int_0^1 \sqrt{\frac{1 + \mu^2 + \psi^2 x^2}{1 - x^2}} dx = n\pi\epsilon, \quad n = 1, 2, \dots \end{aligned} \quad (3.18)$$

The computation of the correction  $\epsilon\theta_1$  is more involved. Note that it is, in principle, needed to obtain a leading-order approximation to the growth rate  $\text{Re } \sigma$  as a function of  $e$  and  $\mu$ . This is because the error on  $\alpha$  needs to be  $o(\epsilon)$ , which requires to approximate the resonance values of  $e$  and  $\mu$  with an  $o(\epsilon)$  error also. We do not pursue these detailed computations here: since the values of  $e$  and  $\mu$  satisfying the resonance condition (3.17) are  $\epsilon$ -close together, Eq. (3.11) provides a useful approximation to the growth rates of the instability without the need to locate the resonances accurately. This is demonstrated in Sec. IV where we compare the prediction (3.11) with numerical solutions of the Floquet problem associated with Eq. (2.8).

Note that the instability-band width can be deduced directly from expression (3.18) for  $\theta_0$ . For fixed  $\epsilon$  and  $e$ , for instance,  $T$  in Eq. (3.9) can be written as  $T = \epsilon^{-1} \Delta\mu \partial_\mu \theta$ , where  $\Delta\mu$  is the distance between  $\mu$  and the resonant values, and the derivative is evaluated at resonance. According to Eq. (3.10), the instability bandwidth is therefore  $\Delta\mu = 2\epsilon |S| / \partial_\mu \theta$ , where  $\theta$  can be approximated by  $\theta_0$ .

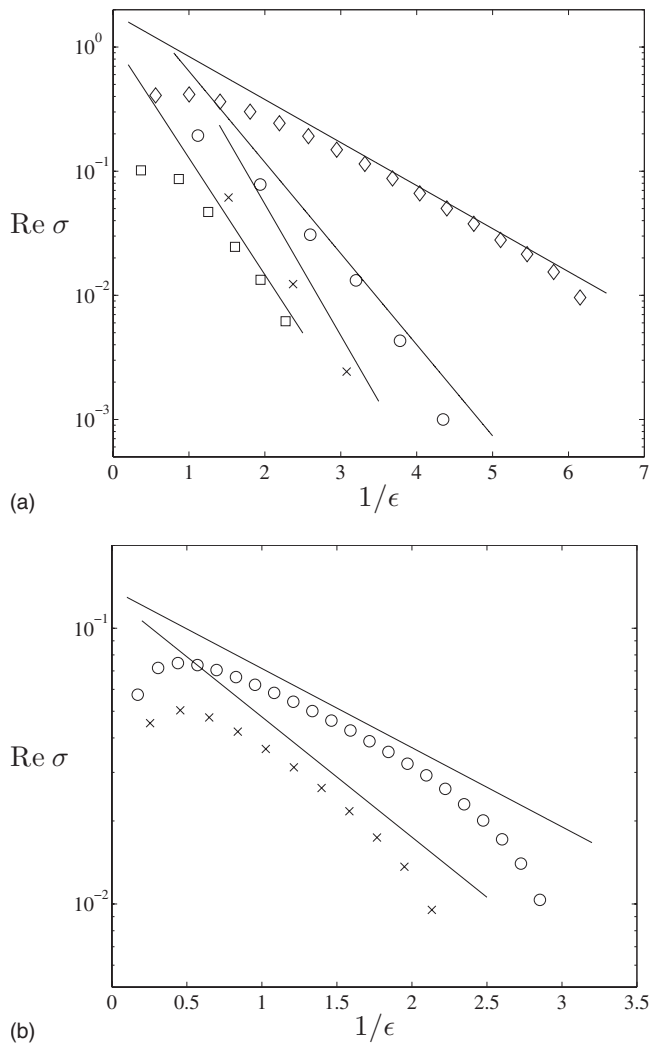


FIG. 2. Numerical estimates of the local maxima of the growth rates  $\text{Re } \sigma$  as functions of the inverse Rossby number  $1/\epsilon$ . (a) Anticyclonic flows with  $e=1.5$ ,  $\mu=1$  ( $\times$ );  $e=2$ ,  $\mu=1$  ( $\circ$ );  $e=2$ ,  $\mu=0.5$  ( $\square$ ); and  $e=4$ ,  $\mu=1$  ( $\diamond$ ). (b) Cyclonic flows with  $e=4$ ,  $\mu=0.5$  ( $\times$ ); and  $e=6$ ,  $\mu=0.5$  ( $\circ$ ). The straight lines in these linear-logarithmic plots indicate the exponential dependence predicted by asymptotic estimate (3.11).

#### IV. COMPARISON WITH NUMERICAL RESULTS

We have solved the Floquet problem associated with Eq. (2.10) for the amplitude  $\zeta$  numerically using MATLAB's standard Runge–Kutta solver. The growth rates  $\text{Re } \sigma$  obtained in this manner are compared to the asymptotic estimate (3.11) for  $\sigma_{\max}$ . To emphasize the exponential dependence on the inverse Rossby number  $1/\epsilon$ , it is convenient to display  $\text{Re } \sigma$  as a function of  $1/\epsilon$  for fixed values of  $\mu$  and of  $e$ . Figures 2(a) and 2(b) summarize the results obtained for several anticyclonic vortices (with  $\varsigma=1$ ) and cyclonic vortices ( $\varsigma=-1$ ), respectively. They display in linear-logarithmic coordinates the local maxima of the growth rates obtained numerically as  $\epsilon$  is varied. The corresponding asymptotic predictions (3.11) are shown as line segments. The maximum growth rates displayed correspond to resonant values of  $1/\epsilon$  for fixed  $e$  and  $\mu$ . Figures 3 and 4 illustrate the complete structure of the instability bands that surround the resonant values by showing all the nonzero growth rates obtained nu-

merically, in linear coordinates and for the parameters of Figs. 2(a) and 2(b), respectively.

The figures confirm the validity of our asymptotic estimate. They also suggest that this estimate remains useful for moderately small values of  $\epsilon$ , say  $\epsilon \leq 1/2$ . Note that the dimensional growth rates are obtained by multiplying  $\sigma$  by  $\sqrt{ab}$  which is related to the relative vorticity  $|\Omega|=a+b$  of the flow by  $\sqrt{ab}=|\Omega|/(e+e^{-1})$ . As expected from our asymptotics, the growth rates in the case of cyclonic flows are exceedingly small for  $\epsilon \ll 1$  even for the large eccentricities used in Fig. 4. Nonetheless, our results clarify the fact that all elliptical flows are unstable, regardless of the sense of the rotation, of its strength, and of the strength of the stratification. Note that the match between asymptotic and numerical results appears to degrade for small  $\epsilon$  (i.e., large  $1/\epsilon$ ), especially for cyclonic flows; this is because the smallness of both the growth rate and instability bandwidth makes the maximum growth rate delicate to estimate numerically. In particular, the agreement between asymptotic and numerical result could be improved by using a finer resolution in  $1/\epsilon$ .

The separation between instability bands can be estimated from the asymptotic formula (3.18): in terms of the varying  $1/\epsilon$  used in the figures, it is given by

$$\gamma = \frac{\pi\mu}{2\int_0^1 \sqrt{\frac{1+\mu^2+\psi^2 x^2}{1-x^2}} dx}.$$

Evaluating this quantity for the parameters chosen for the figures gives  $\gamma=0.62, 0.54, 0.31$ , and  $0.34$  for the parameters of Figs. 3(a)–3(d), and  $\gamma=0.18$  and  $0.12$  for the parameters of Figs. 4(a) and 4(b), in good agreement with the numerical results.

Our derivation of an asymptotic expression for the growth rate makes the hydrostatic approximation, which assumes that  $N \gg f$ ,  $m_0 \gg k_0$ , and  $\mu = fm_0/(Nk_0) = O(1)$ . This assumption, which could be relaxed, is made because it corresponds to the regime most relevant to atmospheric and oceanic flows; it is consistent in the sense that the growth rates obtained are maximized for  $\mu = O(1)$  and decay rapidly for  $\mu \gg 1$  or  $\mu \ll 1$ . To test the sensitivity of the results to the hydrostatic approximation, we have solved the Floquet problem numerically for the full, unapproximated Eq. (2.6) for moderately large values of  $N/f$  and  $m_0/k_0$ . The results obtained for  $\mu=1$  and  $e=4$  are displayed in Fig. 5. This compares the growth rate obtained in the hydrostatic approximation with those obtained for  $N/f=m_0/k_0=3$  and  $6$ . Except for  $\epsilon \gg 1$ , there is relatively little difference between the results: The maximum growth rates fall on the same curve, well described by the hydrostatic asymptotics. Of course, the location of the instability bands changes depending on  $S$ , but this is not significant since they would also change if  $m_0/k_0$  was varied independently of  $N/f$ , as is physically relevant.

#### ACKNOWLEDGMENTS

The authors acknowledge the support of the Network “Wave-Flow Interactions” funded by the UK Engineering and Physical Sciences Research Council. J.M.A. was sup-



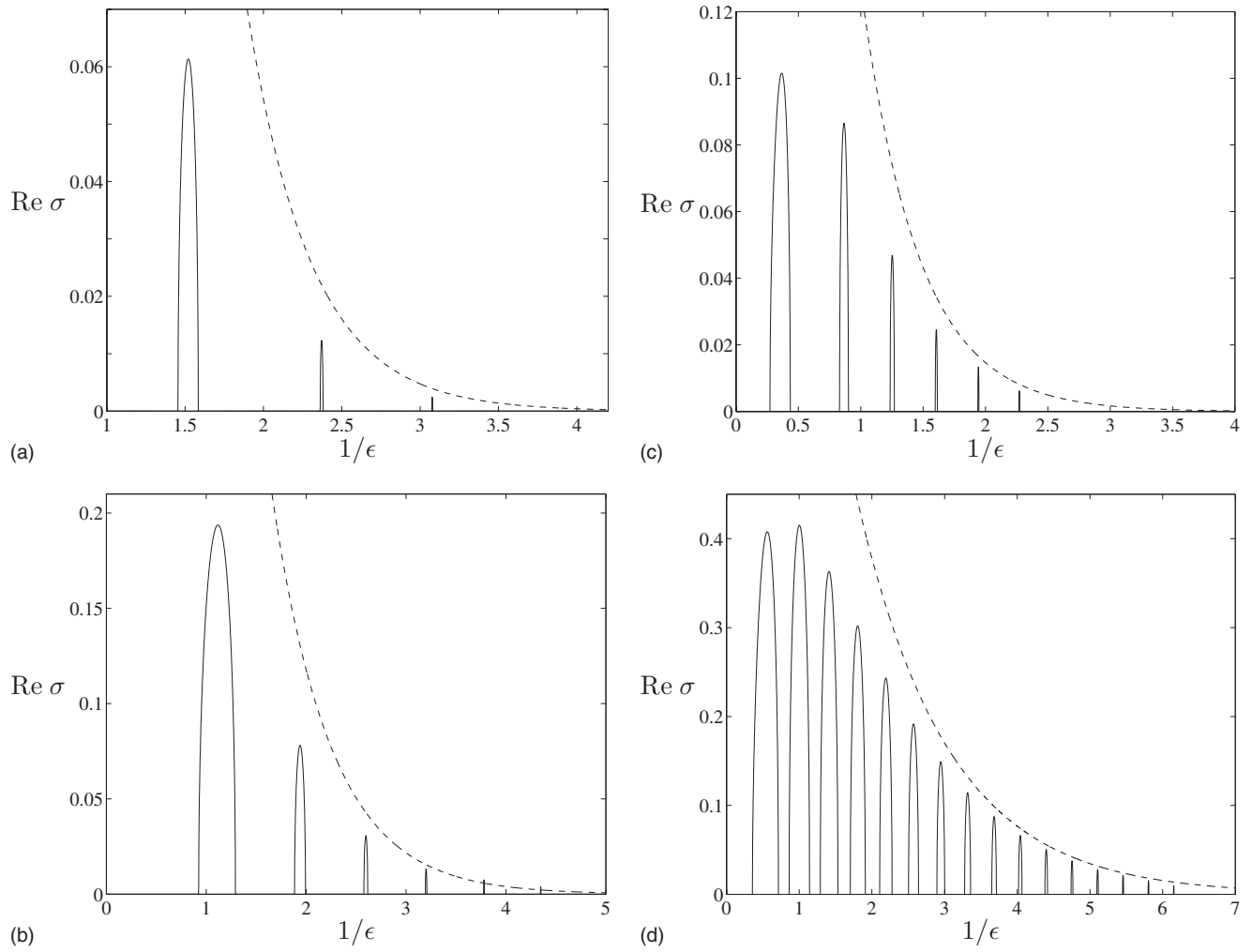


FIG. 3. Growth rates  $\text{Re } \sigma$  in anticyclonic flows as functions of the inverse Rossby number  $1/\epsilon$  for (a)  $e=1.5$ ,  $\mu=1$ ; (b)  $e=2$ ,  $\mu=1$ ; (c)  $e=2$ ,  $\mu=0.5$ ; and (d)  $e=4$ ,  $\mu=1$ . The growth rates computed numerically (solid lines) are compared with the asymptotic estimate of the maximum growth rates  $\sigma_{\max}$  (dashed lines).

ported by a studentship of the UK Natural Environment Research Council.

## APPENDIX A: DERIVATION OF EQUATION (2.6)

The equations that govern an inviscid stratified Boussinesq fluid rotating with constant Coriolis frequency  $f$  are

$$D_t u - f v = -p_x, \quad (\text{A1})$$

$$D_t v + f u = -p_y, \quad (\text{A2})$$

$$D_t w + \rho = -p_z, \quad (\text{A3})$$

$$D_t \rho - N^2 w = 0, \quad (\text{A4})$$

$$u_x + v_y + w_z = 0, \quad (\text{A5})$$

where  $(u, v, w)$  are the usual Cartesian velocity components and  $D_t = \partial_t + u \partial_x + v \partial_y + w \partial_z$  is the material derivative. The variable  $\rho$  is a scaled density, such that the total density is given by

$$\rho_{\text{tot}} = \rho_b + \frac{\rho_b}{g} [-N^2 z + \rho(x, y, z, t)], \quad (\text{A6})$$

where  $\rho_b$  is the uniform background density, and  $N$  is the Brunt–Väisälä frequency. The Boussinesq approximation assumes that  $|\rho_{\text{tot}} - \rho_b| \ll \rho_b$ .

We seek solutions that are the sum of the elliptical flow (2.1) and the small-amplitude plane wave with time-dependent wavevector (2.3). Thus we introduce the decomposition

$$(u, v, w, \rho, p) = (ay, -bx, 0, 0, b(a-f)x^2/2 + a(b-f)y^2/2) + (\hat{u}(t), \hat{v}(t), \hat{w}(t), \hat{\rho}(t), \hat{p}(t)) e^{ik(t) \cdot x} \quad (\text{A7})$$

into Eqs. (A1)–(A5) and linearize the resulting equations. Imposing that the wavevector components satisfy Eq. (2.4) eliminates the terms that depend explicitly on  $x$  and  $y$ , leaving a system of five ordinary differential equations for  $[\hat{u}(t), \hat{v}(t), \hat{w}(t), \hat{\rho}(t), \hat{p}(t)]$ . This system is simplified by introducing the amplitudes of the vertical component of vorticity  $\hat{\zeta} = ik\hat{v} - il\hat{u}$  and of the horizontal divergence  $\hat{\delta} = ik\hat{u} + il\hat{v}$ . These amplitudes are found to satisfy

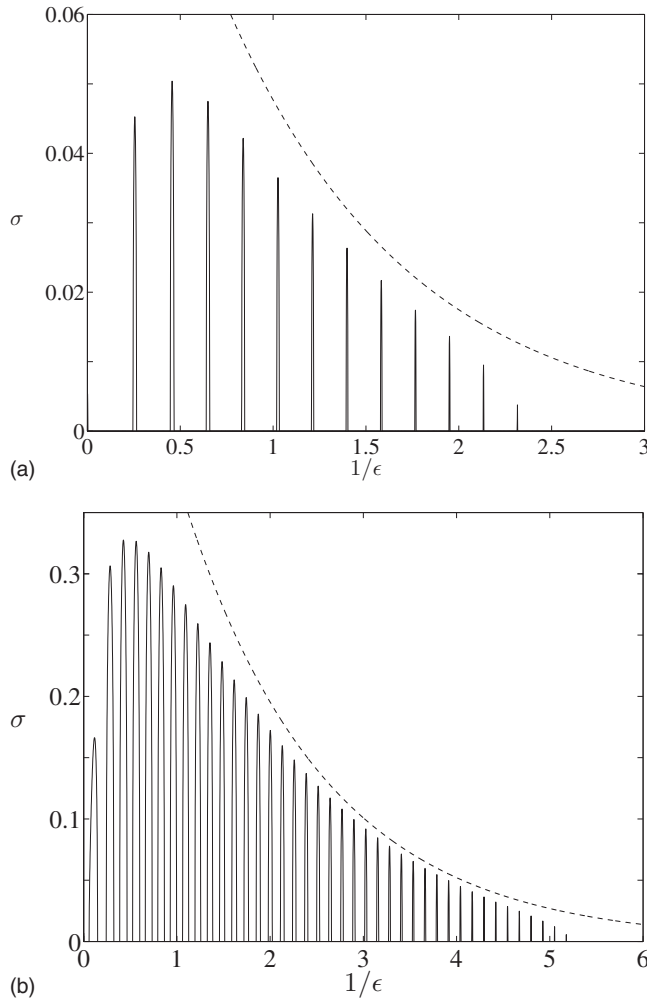


FIG. 4. Growth rates  $\text{Re } \sigma$  in cyclonic flows as functions of the inverse Rossby number  $1/\epsilon$  for (a)  $e=4$ ,  $\mu=0.5$ ; and (b)  $e=6$ ,  $\mu=0.5$ . The growth rates computed numerically (solid lines) are compared to the asymptotic estimate of the maximum growth rates  $\sigma_{\max}$  (dashed lines).

$$\dot{\hat{\zeta}} = (a + b - f)\hat{\delta}, \quad (\text{A8})$$

$$\begin{aligned} \dot{\hat{\delta}} = & \frac{i(k^2 + l^2)}{m}(\hat{\rho} + \hat{w}) + \left(f - \frac{2(k^2 a + l^2 b)}{k^2 + l^2}\right)\hat{\zeta} \\ & + \frac{2(b-a)kl}{k^2 + l^2}\hat{\delta}. \end{aligned} \quad (\text{A9})$$

The vertical velocity  $\hat{w}$  can be eliminated from Eq. (A9) using that  $\hat{\delta} + im\hat{w} = 0$ . To eliminate the density  $\hat{\rho}$ , we first obtain the conservation  $\dot{\hat{q}} = 0$  for the (scaled) potential vorticity  $\hat{q} = N^2 \hat{\zeta} + i(a+b-f)m\hat{\rho}$ . Assuming that  $\hat{q}(t) = \hat{q}(0) = 0$  then reduces Eqs. (A8) and (A9) to two coupled equations for  $\hat{\zeta}$  and  $\hat{\delta}$ , respectively. Eliminating  $\hat{\delta}$  and removing the hat of  $\zeta$  finally leads to Eq. (2.6).

## APPENDIX B: EXPONENTIAL ASYMPTOTICS

In this appendix, we compute the (exponentially small) Stokes multiplier  $S$  which quantifies the switching on of one branch of the WKB solution by the other [see Eqs. (3.6) and (3.7)] through a Stokes phenomenon.<sup>14,18</sup> The Stokes phe-

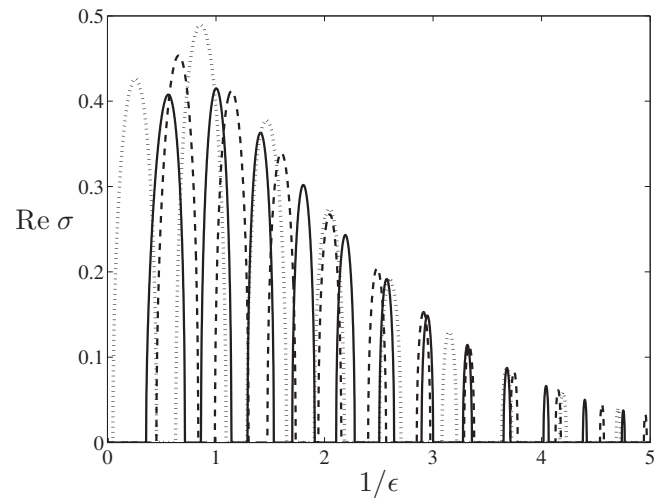


FIG. 5. Effect of the hydrostatic approximation: The growth rate  $\text{Re } \sigma$  is plotted as a function of the inverse Rossby number  $1/\epsilon$  for an anticyclonic flow with  $e=4$  and  $\mu=1$ , in the hydrostatic limit  $N/f \rightarrow \infty$  (solid lines), for  $N/f=6$  (dashed lines), and for  $N/f=3$  (dotted lines).

nomenon is associated with the presence of complex turning points, that is, complex times where  $\omega=0$ . From Eq. (2.11), these are located at

$$t_n = i \sinh^{-1} \frac{\sqrt{1+\mu^2}}{\psi} + n\pi, \quad n = 0, \pm 1, \pm 2, \dots$$

and  $\bar{t}_n$ . The Stokes phenomenon occurs across Stokes lines, which are defined by  $\text{Re} \int_{t_n}^t \omega(t') dt' = 0$ . Our interest is in the Stokes lines crossing the interval  $[-\pi/2, \pi/2]$ . It is easy to see that the segment of  $\text{Re } t=0$  joining  $t_0$  to  $\bar{t}_0$  is such a Stokes line; it is also the only one since for  $-\pi/2 < t < \pi/2$ ,  $\text{Re} \int_{t_0}^t \omega(t') dt' = \text{Re} \int_0^t \omega(t') dt' = \int_0^t \omega(t') dt' \neq 0$  unless  $t=0$ .

We compute  $S$  using matched asymptotics, examining how the solution  $\zeta = A(t) \exp[i\theta(t)/\epsilon]$  connects to the solution  $\zeta = A(t) \{ \exp[i\theta(t)/\epsilon] + S \exp[-i\theta(t)/\epsilon] \}$  as this segment is crossed.<sup>21</sup> To analyze the behavior of the solution in the neighborhood of  $t_0$ , we first note that

$$\begin{aligned} \omega & \sim a^{1/2} e^{i\pi/4} (t - t_0)^{1/2}, \quad \text{where} \\ a & = \sqrt{2(1+\mu^2)(1+\psi^2+\mu^2)}/\mu^2, \end{aligned} \quad (\text{B1})$$

as  $t \rightarrow t_0$ . We then rescale the evolution equation for  $\zeta$  near  $t_0$  by defining the inner variables

$$\tau = \epsilon^{-2/3} a^{1/3} (t - t_0) \quad \text{and} \quad Z(\tau) = \zeta(t).$$

Retaining only the leading-order terms, this transforms Eq. (2.10) into the equation

$$\frac{d^2 Z}{d\tau^2} + i\tau Z = 0. \quad (\text{B2})$$

Solutions can be written in terms of the Airy functions  $\text{Ai}(e^{-i\pi/6}\tau)$  and  $\text{Bi}(e^{-i\pi/6}\tau)$ . We claim that the solution of interest is

$$Z \sim C[\text{Ai}(e^{-i\pi/6}\tau) + i \text{Bi}(e^{-i\pi/6}\tau)]. \quad (\text{B3})$$

We verify that this solution matches  $A(t)\exp[i\theta(t)/\epsilon]$  to the left of the Stokes line  $\text{Re } t=0$ ; in doing so we find an expression for the constant  $C$ . It is convenient to verify the matching along the line  $\text{ph } \tau = -5\pi/6$ ; this is an anti-Stokes line along which the two independent solutions of Eq. (B2) have similar orders of magnitudes. Along this line, we can use the asymptotic formulas<sup>24</sup>

$$\text{Ai}(-z) \sim \frac{1}{\sqrt{\pi z^{1/4}}} \cos(2z^{3/2}/3 - \pi/4), \quad (\text{B4})$$

$$\text{Bi}(-z) \sim -\frac{1}{\sqrt{\pi z^{1/4}}} \sin(2z^{3/2}/3 - \pi/4), \quad (\text{B5})$$

with  $z = -\exp(-i\pi/6)\tau = \exp(5i\pi/6)\tau \rightarrow +\infty$ . Thus we have

$$Z \sim \frac{C e^{i\pi/24}}{\sqrt{\pi \tau^{1/4}}} e^{2ie^{i\pi/4}\tau^{3/2/3}}. \quad (\text{B6})$$

On the other hand, using Eqs. (3.4) and (3.5) the solution  $\zeta = A(t)\exp[i\theta(t)]$ , valid in the outer region away from  $t_0$  and to the left of the Stokes line  $\text{Re } t=0$ , can be written as

$$\begin{aligned} \zeta &\sim \frac{1}{\omega^{1/2}} e^{\int_{-\pi/2}^t p(t') dt'/2} e^{i\epsilon^{-1} \int_{-\pi/2}^t \{\omega(t') - \epsilon q(t')/[2\omega(t')]\} dt'} \\ &\sim \frac{e^{-i\pi/8}}{(\epsilon a)^{1/6} \tau^{1/4}} e^{\int_{\Gamma_-} p(t') dt'/2} e^{i\epsilon^{-1} \int_{\Gamma_-} \{\omega(t') - \epsilon q(t')/[2\omega(t')]\} dt'} \\ &\quad \times e^{2ie^{i\pi/4}\tau^{3/2/3}}, \end{aligned} \quad (\text{B7})$$

after using Eq. (B1). Here  $\Gamma_-$  denotes a contour joining  $-\pi/2$  to  $t_0$  while remaining to the left of the Stokes line  $\text{Re } t=0$ . Comparing Eq. (B7) with Eq. (B6) shows that  $\zeta$  correctly matches  $Z$  provided that

$$C = \frac{\sqrt{\pi} e^{-i\pi/6}}{(\epsilon a)^{1/6}} e^{\int_{\Gamma_-} p(t') dt'/2} e^{i\epsilon^{-1} \int_{\Gamma_-} \{\omega(t') - \epsilon q(t')/[2\omega(t')]\} dt'}. \quad (\text{B8})$$

We now match  $Z$  with the outer solution valid to the right of the Stokes line  $\text{Re } t=0$ . A connection formula for Airy functions<sup>24</sup> gives the alternative form

$$Z \sim 2C e^{i\pi/3} \text{Ai}(e^{-i5\pi/6}\tau), \quad (\text{B9})$$

for Eq. (B3). Carrying out the matching on the anti-Stokes line  $\text{ph } \tau = \exp(-i\pi/6)$ , we can use the asymptotic formula for Ai in Eq. (B4) to write that

$$Z \sim \frac{C e^{i\pi/24}}{\sqrt{\pi \tau^{1/4}}} (e^{2ie^{i\pi/4}\tau^{3/2/3}} + i e^{-2ie^{i\pi/4}\tau^{3/2/3}}) \quad (\text{B10})$$

for  $|\tau| \rightarrow \infty$ . This should be matched with the form  $\zeta(t) = A(t)\{\exp[i\theta(t)/\epsilon] + S \exp[-i\theta(t)/\epsilon]\}$  of the solution to the right of the Stokes line. Using Eq. (B1) gives the asymptotics

$$\begin{aligned} \zeta &\sim \frac{1}{\omega^{1/2}} e^{\int_{-\pi/2}^t p(t') dt'/2} \left[ e^{i\epsilon^{-1} \int_{-\pi/2}^t \{\omega(t') - \epsilon q(t')/[2\omega(t')]\} dt'} \right. \\ &\quad \left. + S e^{-i\epsilon^{-1} \int_{-\pi/2}^t \{\omega(t') - \epsilon q(t')/[2\omega(t')]\} dt'} \right] \\ &\sim \frac{e^{-i\pi/8}}{(\epsilon a)^{1/6} \tau^{1/4}} e^{\int_{\Gamma_+} p(t') dt'/2} \\ &\quad \times \left[ e^{i\epsilon^{-1} \int_{\Gamma_+} \{\omega(t') - \epsilon q(t')/[2\omega(t')]\} dt'} e^{2ie^{i\pi/4}\tau^{3/2/3}} \right. \\ &\quad \left. + S e^{-i\epsilon^{-1} \int_{\Gamma_+} \{\omega(t') - \epsilon q(t')/[2\omega(t')]\} dt'} e^{-2ie^{i\pi/4}\tau^{3/2/3}} \right], \end{aligned}$$

where  $\Gamma_+$  denotes a contour joining  $-\pi/2$  to  $t_0$ . This contour crosses the Stokes line  $\text{Re } t=0$  below the singular point  $t_p$  of  $p(t)$  and  $q(t)$ , given by  $t_p = i \sinh^{-1}(1/\psi)$ . Taking Eq. (B8) into account, the matching with Eq. (B10) gives the two equations

$$e^{\int_{\Gamma_-} p(t) dt/2} e^{-i \int_{\Gamma_-} q(t)/\omega(t) dt/2} = e^{\int_{\Gamma_+} p(t) dt/2} e^{-i \int_{\Gamma_+} q(t)/\omega(t) dt/2}, \quad (\text{B11})$$

$$\begin{aligned} i e^{\int_{\Gamma_-} p(t') dt'/2} e^{i\epsilon^{-1} \int_{\Gamma_-} \{\omega(t') - \epsilon q(t')/[2\omega(t')]\} dt'} \\ = S e^{\int_{\Gamma_+} p(t') dt'/2} e^{-i\epsilon^{-1} \int_{\Gamma_+} \{\omega(t') - \epsilon q(t')/[2\omega(t')]\} dt'}. \end{aligned} \quad (\text{B12})$$

We can now deform the integration contours. The difference  $\int_{\Gamma_+} - \int_{\Gamma_-}$  reduces to an integral along a closed contour encircling  $t_p$ . Computing the corresponding residues using Eq. (2.12) gives

$$\text{Res}_{t_p} p = 1 \quad \text{and} \quad \text{Res}_{t_p} \frac{q}{\omega} = -is.$$

Taking this into account confirms that Eq. (B11) is an identity. Using  $\text{Res}_{t_p} p = 1$  in Eq. (B12) gives the Stokes multiplier as

$$S = -ie^{2i\epsilon^{-1} \int_{-\pi/2}^{t_0} \{\omega(t') - \epsilon q(t')/[2\omega(t')]\} dt'},$$

where the Cauchy principal value integral, denoted by  $\oint$ , is necessary because  $q(t)$  has a pole at  $t=t_p$ . It follows that  $|S|$ , giving the instability growth rate, can be written as

$$|S| = e^{-\alpha/\epsilon + s\beta},$$

where the two constants

$$\alpha = -2i \int_0^{t_0} \omega(t) dt \quad \text{and} \quad \beta = -i \oint_0^{t_0} \frac{sq(t)}{\omega(t)} dt$$

are real, positive and independent of  $s$ . Using Eqs. (2.11) and (2.12), they can be given the more explicit forms

$$\alpha = \frac{2}{\mu} \int_0^{\sinh^{-1}(\sqrt{1+\mu^2}/\psi)} \sqrt{1 - \psi^2 \sinh^2 u + \mu^2} du,$$

and

$$\begin{aligned} \beta &= \mu s \int_0^{\sinh^{-1}(\sqrt{1+\mu^2}/\psi)} \left( e + e^{-1} + \frac{2e}{1 - \psi^2 \sinh^2 u} \right) \\ &\quad \times \frac{du}{\sqrt{1 - \psi^2 \sinh^2 u + \mu^2}}, \end{aligned}$$

and further transformed into the convenient expressions (3.13) and (3.14).

- <sup>1</sup>R. R. Kerswell, "Elliptical instability," *Annu. Rev. Fluid Mech.* **34**, 83 (2002).
- <sup>2</sup>T. Miyazaki, "Elliptical instability in a stably stratified rotating fluid," *Phys. Fluids A* **5**, 2702 (1993).
- <sup>3</sup>S. Leblanc, "Internal wave resonances in strain flows," *J. Fluid Mech.* **477**, 259 (2003).
- <sup>4</sup>J. C. McWilliams and I. Yavneh, "Fluctuation growth and instability associated with a singularity of the balance equations," *Phys. Fluids* **10**, 2587 (1998).
- <sup>5</sup>M. J. Molemaker, J. C. McWilliams, and I. Yavneh, "Baroclinic instability and loss of balance," *J. Phys. Oceanogr.* **35**, 1505 (2005).
- <sup>6</sup>J. Vanneste and I. Yavneh, "Unbalanced instabilities of rapidly rotating stratified shear flows," *J. Fluid Mech.* **584**, 373 (2007).
- <sup>7</sup>J. C. McWilliams, M. J. Molemaker, and I. Yavneh, "Ageostrophic, anticyclonic instability of a geostrophic, barotropic boundary current," *Phys. Fluids* **16**, 3720 (2004).
- <sup>8</sup>R. Plougonven, D. J. Muraki, and C. Snyder, "A baroclinic instability that couples balanced motions and gravity waves," *J. Atmos. Sci.* **62**, 1545 (2005).
- <sup>9</sup>Note that we use the conventional form of Rossby number rather than its inverse as used in Ref. 2.
- <sup>10</sup>J. Vanneste and I. Yavneh, "Exponentially small inertia-gravity waves and the breakdown of quasi-geostrophic balance," *J. Atmos. Sci.* **61**, 211 (2004).
- <sup>11</sup>J. Vanneste, "Exponential smallness of inertia-gravity-wave generation at small Rossby number," *J. Atmos. Sci.* **65**, 1622 (2008).
- <sup>12</sup>C. M. Bender and S. A. Orszag, *Advanced Mathematical Methods for Scientists and Engineers* (Springer, New York, 1999).
- <sup>13</sup>M. I. Weinstein and J. B. Keller, "Asymptotic behaviour of stability regions for Hill's equation," *SIAM J. Appl. Math.* **47**, 941 (1987).
- <sup>14</sup>M. J. Ablowitz and A. S. Fokas, *Complex Variables: Introduction and Applications* (Cambridge University Press, Cambridge, 1997).
- <sup>15</sup>S. J. Friedlander and A. Lipton-Lifschitz, in *Handbook of Mathematical Fluid Dynamics*, edited by S. J. Friedlander and D. Serre (Elsevier Science, New York, 2003), Vol. 2, pp. 289–353.
- <sup>16</sup>S. Le Dizès, "Three-dimensional instability of a multipolar in a rotating flow," *Phys. Fluids* **12**, 2762 (2000).
- <sup>17</sup>D. Guimbard and S. Leblanc, "Local stability of the Abrashkin–Yakubovich family of vortices," *J. Fluid Mech.* **567**, 91 (2006).
- <sup>18</sup>R. B. Paris and A. D. Wood, "Stokes phenomenon demystified," *Bull. Inst. Math. Appl.* **31**, 21 (1995).
- <sup>19</sup>M. V. Berry, "Uniform asymptotic smoothing of Stokes's discontinuities," *Proc. R. Soc. London, Ser. A* **422**, 7 (1989).
- <sup>20</sup>*Asymptotics Beyond All Orders*, edited by H. Segur, S. Tanveer, and H. Levine (Plenum, New York, 1991).
- <sup>21</sup>V. Hakim, "Asymptotic techniques in nonlinear problems: Some illustrative examples," in *Hydrodynamics and Nonlinear Instabilities*, edited by C. Godrèche and P. Manneville (Cambridge University Press, Cambridge, 1998), Chap. 3, pp. 295–386.
- <sup>22</sup>A. B. Olde Daalhuis, S. J. Chapman, J. R. King, J. R. Ockendon, and R. H. Tew, "Stokes phenomenon and matched asymptotic expansions," *SIAM J. Appl. Math.* **55**, 1469 (1995).
- <sup>23</sup>This can be related to the fact that  $\det M = 1$  which follows from the periodicity of the Wronskian  $W$  and implies that instability arises when the  $\lambda$  are purely real. However, they are complex conjugate to all orders in  $\epsilon$ , a property which persists in the presence of a small perturbation in the nondegenerate cases  $\lambda \neq \pm 1 + O(S)$ .
- <sup>24</sup>M. Abramowitz and I. A. Stegun, *Handbook of Mathematical Functions* (Dover, New York, 1965).